

Biexcitons bound to single-island interface defects

O. Heller, Ph. Lelong, and G. Bastard

Laboratoire de Physique de la Matière Condensée, Ecole Normale Supérieure, 24 rue Lhomond, 75005 Paris, France

(Received 28 January 1997)

We calculate the binding energy of biexcitons bound to single-island interface defects in deep quantum wells. The application of a variational function leads to a calculation that is mostly analytical. We discuss in detail the dependence of the biexciton binding energy on the defect size and the quantum-well width. The numerical calculations are carried out for $\text{Al}_x\text{Ga}_{1-x}\text{As}/\text{GaAs}$ quantum wells with defect depths of 1 and 2 monolayers corresponding to recent experimental findings. Furthermore, we attempt to correlate our problem of a localized biexciton with the existing results for free four-particle molecules in different confinement structures and for different mass ratios. [S0163-1829(97)03932-5]

I. INTRODUCTION

Nonlinear optical experiments allow the study of molecules of two excitons called biexcitons. Due to the complexity of the biexciton wave function, the effort and the number of methods for the calculation of the biexcitonic energy are continuously increasing. The most general one is the variational method, which is applicable to all kinds of quantum structures that are large compared to the lattice constant. For bulk biexcitons this method was employed by Brinkman *et al.*,¹ followed by Miller *et al.*² and Kleinman³ for quantum wells (QW's). Quantum-well wires,^{4,5} (QWW's) and quantum dots⁶ (QD's) have also been examined successfully. A second method consists in a perturbative analysis. In order to obtain a discrete electronic spectrum this method has been applied to QD's with infinite-barrier potentials and sizes smaller than the exciton Bohr radius. Bryant⁷ has studied finite dots, whereas Bányai⁸ has analyzed the limit of vanishing dot size up to the second order. In the case of finite QD's with infinite barriers one of the most accurate procedure is the numerical matrix diagonalization,^{9,10} which uses the unperturbed electronic wave functions as a basis for the excitonic and biexcitonic wave functions. Due to the large number of integration dimensions, quantum Monte Carlo calculations found a way in this domain. It was demonstrated that this method is also reliable^{11,12} by a comparison between its predictions and those of the perturbative matrix diagonalization. Finally, there has been an application of the fractional dimension approach to biexcitons in QW's by Birkedal *et al.*¹³

Parallel to the investigations of biexcitons in semiconductor physics, the corresponding molecules of two hydrogen or positronium atoms have been studied in molecular physics. The most recent and very powerful calculations consist in a combination of a variational calculation for a set of Gaussian functions¹⁴ or modern Hylleraas-type wave functions.¹⁵

Recently $\text{Al}_x\text{Ga}_{1-x}\text{As}/\text{GaAs}$ QW's with single-island interface defects formed by monolayer fluctuations of the QW width have been studied experimentally. This kind of interface defect creates a lateral potential and thus localizes excitons. It acts therefore as a natural quantum dot. Sharp photoluminescence lines below the localized exciton have been observed and attributed to localized biexcitons.¹⁶ In

$\text{ZnSe}/\text{Zn}_x\text{Cd}_{1-x}\text{Se}$ QW's biexcitons localized to alloy disorder have been detected.^{17,18} On the theoretical side, a model for lasing oscillations due to localized biexcitons has been developed.¹⁹

We present in this paper calculations of the binding energies of the localized excitons and biexcitons by using the variational method. In this case no convenient approach with infinite barriers can be chosen. Consequently, the perturbative and the matrix diagonalization methods are excluded because the interface defect has only a few bound electronic states.²⁰ The paper is arranged as follows. In Sec. II we discuss the properties of an exciton bound to an interface defect by the use of two different trial wave functions. The exciton binding energy and the lateral exciton extension are analyzed in detail. In Sec. III we investigate the same quantities for the biexciton. We also present a comparison of the bound biexcitons with free bulk and free quantum-well biexcitons. In both sections we show numerical results for a $\text{Al}_x\text{Ga}_{1-x}\text{As}/\text{GaAs}$ QW as a function of the defect size for defect depths of 1 and 2 monolayers (ML). Furthermore, we analyze the ratio of the attractive and repulsive Coulomb energies in the biexciton and compare it with the results for the free hydrogen and the free positronium molecule. We summarize our results in Sec. IV and present the analytical calculations of the most difficult terms in the Appendix.

II. EXCITON

For the exciton we take the well-known Hamiltonian²¹ for the QW with a width L centered at $z = 0$ and add the binding energy \mathcal{V}_{def} due to the interface defect. The defect is assumed to have a cylindrical symmetry with a lateral radius D and to be centered at $\varrho = 0$. Its extension in the z direction is A and the potential depth corresponds to the barrier potential $U_e = x \times 770$ meV ($U_h = x \times 480$ meV) for the electron (hole) and therefore depends on the Al concentration x of the barrier:

$$\mathcal{H} = \mathcal{H}_{QW} + \mathcal{V}_{def}(e) + \mathcal{V}_{def}(h),$$

$$\mathcal{H}_{QW} = \mathcal{H}_e + \mathcal{H}_h + \mathcal{T}_{xy} + \mathcal{H}_{Coul}, \quad (1)$$

$$\mathcal{V}_{def}(e, h) = -U_{e,h} 1_{[L/2, L/2+A]}(z_{e,h}) e^{-\varrho_{e,h}^2/D^2},$$

where $1_{[a,b]}$ is equal to 1 in the interval $[a,b]$ and 0 otherwise. In the following we will discuss in detail the exciton binding energy to the interface defect $E_{bin}(ex)$, which is defined as the energy difference of the total exciton energy with and without the defect potential. In the case of low barriers and shallow defects the exciton binding energy to the interface defect is small compared to the exciton binding energy and thus compared to the energy distance between the $1s$ and $2s$ states. Consequently, a description of the in-plane exciton ground state by the free exciton term $\Phi_{1s}(\varrho)$ for the relative motion and a further term $\Psi(R)$ for the motion of the center of mass is appropriate.²² This procedure cannot be applied to the case of deep QW's where the binding energy due to the interface defect is of the order of the excitonic binding energy. Instead, we describe the exciton wave function Ψ_{ex} by an excitonic correlation term Θ_{corr} for the relative motion and two independent localization terms Ω_{loc} for the electron and the hole. In order to get a wave function that allows a tractable calculation even for the biexciton we use a Gaussian function in ϱ for the relative motion. Furthermore, we use a separable form for the z direction and the xy plane, which is justified for deep QW's with shallow defects. Our trial wave function thus depends on three variational parameters: λ for the relative exciton motion and λ_e and λ_h for the electron and hole localizations:

$$\begin{aligned} \Psi_{ex} &= N \Omega_{loc}(e, \lambda_e) \Omega_{loc}(h, \lambda_h) \Theta_{corr}(e, h, \lambda), \\ \Omega_{loc}(i, \mu) &= \chi_i(z_i) e^{-\varrho_i^2/\mu^2}, \\ \Theta_{corr}(i, j, \mu) &= e^{-(\vec{\varrho}_i - \vec{\varrho}_j)^2/\mu^2}. \end{aligned} \quad (2)$$

The choice of a Gaussian in ϱ leads to an underestimate of the exciton binding energy, which will be assessed by a comparison with a second trial wave function Φ_{ex} .²³ It consists in the exact three-dimensional numerical solutions ξ_e^0 and ξ_h^0 for the interface defect problem without the Coulomb term. The latter is taken into account by a three-dimensional excitonic correlation term. This approach contains only one excitonic variational parameter μ :

$$\Phi_{ex} = N \xi_e^0(\vec{r}_e) \xi_h^0(\vec{r}_h) e^{-|\vec{r}_e - \vec{r}_h|/\mu}. \quad (3)$$

The system under consideration is an $\text{Al}_x\text{Ga}_{1-x}\text{As}/\text{GaAs}$ QW with a width $L=35$ Å and an aluminium concentration $x=0.35$. Neglecting the mass mismatch, we use for the masses for the electron (e) and the heavy hole (hh) $m_{xy}(e) = m_z(e) = 0.0782m_0$, $m_{xy}(hh) = 0.112m_0$, and $m_z(hh) = 0.377m_0$. The remaining parameters are the same as in Ref. 21. In Fig. 1 we present the exciton binding energy to the interface defect for the hh exciton with interface defects of 1 and 2 ML depths ($A=2.83$ and 5.66 Å).

In the region of very small defect radii Ψ_{ex} is not appropriate: it leads to negative binding energies, whereas Φ_{ex} provides a better description in the whole range due to the three-dimensional excitonic description. In the following we will restrict ourselves to an intermediate defect size region between 100 and 400 Å, which corresponds to the estimated size of interface defects in many samples.

For defect sizes ranging from 100 to 400 Å we get for 1 ML binding energies of 1.4–7.4 meV for Ψ_{ex} and 2.4–

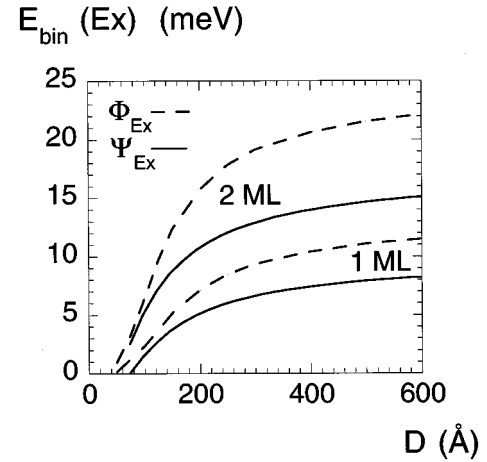


FIG. 1. Exciton binding energy to the interface defect versus defect size D for defect depths of 1 and 2 ML.

10.4 meV for Φ_{ex} and for 2 ML binding energies of 5.1–14.0 meV for Ψ_{ex} and 6.4–20.6 meV for Φ_{ex} . This comparison shows a discrepancy of the order of 30% in this intermediate region. On the experimental side, Brunner *et al.*¹⁶ have found for a comparable $\text{Al}_x\text{Ga}_{1-x}\text{As}/\text{GaAs}$ structure a value of about 12.4 meV for the excitonic binding energy, which indicates a defect depth between 1 and 2 ML.

In order to estimate the lateral extension of the exciton, we have calculated the expectation value for the electron distance from the defect center $\langle \varrho_e \rangle$. The results are shown in Fig. 2. The general trend is a divergence for small defects, a minimum in the intermediate region, and a continuous increase for increasing sizes. The two limits of vanishing and infinitely large defect sizes correspond to the nonlocalized regime of a free QW exciton that has no single-particle lateral length scale. The stronger lateral localization of Ψ_{ex} compared to Φ_{ex} is due to the different treatments of the lateral part. In the case of Ψ_{ex} the lateral parameters λ_e and λ_h are varied, leading to a more or less successful localization to the defect potential, whereas in the case of Φ_{ex} the electronic lateral functions are maintained and only the excitonic

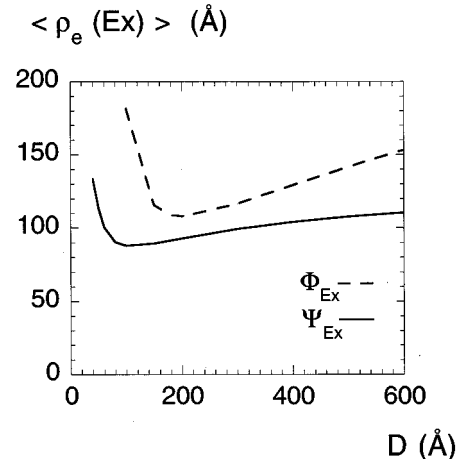


FIG. 2. Excitonic expectation value for the electron lateral distance from the defect center versus defect size D for a defect depth of 1 ML.

parameter is varied. The corresponding expectation values for the hole differ only by a few percent from those of the electron. As a consequence, we can identify $\langle \varrho_e \rangle$ with the lateral exciton size. The important point is that in the intermediate region the localization follows the size of the defect, i.e., for decreasing defect size the exciton size decreases also. This trend of the exciton localization will be compared in the following section with the biexciton localization. For Ψ_{ex} the exciton extension in the intermediate region is of the order of 100 Å and changes only weakly with D .

III. BIEXCITON

The Hamiltonian for a biexciton in a QW with an interface defect is written as

$$\begin{aligned} \mathcal{H} &= \mathcal{H}_{e1} + \mathcal{H}_{e2} + \mathcal{H}_{h1} + \mathcal{H}_{h2} + \mathcal{T}_{xy} + \mathcal{H}_{Coul} + \mathcal{V}_{def}(e_1) \\ &\quad + \mathcal{V}_{def}(e_2) + \mathcal{V}_{def}(h_1) + \mathcal{V}_{def}(h_2), \\ \mathcal{T}_{xy} &= -\frac{\hbar^2}{2m_{xy}^*(e)}(\Delta_{\vec{e}_1} + \Delta_{\vec{e}_2}) - \frac{\hbar^2}{2m_{xy}^*(h)}(\Delta_{\vec{e}_1} + \Delta_{\vec{e}_2}), \\ \mathcal{H}_{Coul} &= \frac{e^2}{4\pi\epsilon_0\epsilon_r} \left[\frac{1}{|\vec{r}_{e1} - \vec{r}_{e2}|} + \frac{1}{|\vec{r}_{h1} - \vec{r}_{h2}|} - \frac{1}{|\vec{r}_{e1} - \vec{r}_{h1}|} \right. \\ &\quad \left. - \frac{1}{|\vec{r}_{e1} - \vec{r}_{h2}|} - \frac{1}{|\vec{r}_{e2} - \vec{r}_{h1}|} - \frac{1}{|\vec{r}_{e2} - \vec{r}_{h2}|} \right]. \quad (4) \end{aligned}$$

A glance at the form of the biexciton Hamiltonian allows one to get some general information on the wave function. First, one deduces from the Coulomb part of the Hamiltonian that the biexciton wave function depends on the difference coordinates. It has to be not only a function of the *attractive coordinates* $|\vec{r}_{e1} - \vec{r}_{h1}|$, $|\vec{r}_{e1} - \vec{r}_{h2}|$, $|\vec{r}_{e2} - \vec{r}_{h1}|$, and $|\vec{r}_{e2} - \vec{r}_{h2}|$ but also of the *repulsive coordinates* $|\vec{r}_{e1} - \vec{r}_{e2}|$ and $|\vec{r}_{h1} - \vec{r}_{h2}|$. Second, the interface defect potential-energy part requires a further dependence on the single-particle coordinates $\varrho_{e1}, \varrho_{e2}, \varrho_{h1}, \varrho_{h2}$, which accounts for the localization. For the ground state we choose a wave function that is totally symmetric in the space part and totally antisymmetric in the spin part, which corresponds to the spin singlet state for both the electrons and holes. We take the product of two exciton wave functions Ψ_{ex} of Sec. II and symmetrize it by adding the permuted function Ψ_2 :

$$\begin{aligned} \Psi_{bi} &= N\Omega_{loc}(e_1, \lambda_e)\Omega_{loc}(e_2, \lambda_e)\Omega_{loc}(h_1, \lambda_h)\Omega_{loc}(h_2, \lambda_h) \\ &\quad \times [\Theta_{corr}(e_1, h_1, \lambda)\Theta_{corr}(e_2, h_2, \lambda) \\ &\quad + \Theta_{corr}(e_1, h_2, \lambda)\Theta_{corr}(e_2, h_1, \lambda)] \\ &= \Psi_1 + \pi_e(1,2)\Psi_1 \\ &= \Psi_1 + \Psi_2. \quad (5) \end{aligned}$$

The idea of taking advantage of the tractability of the Gaussian functions has already been used by Rebane and Zotev¹⁴ for the positronium molecule. They used correlation terms not only for the attractive coordinates but also for the repulsive ones. In their case the calculation is completely analytical due to the fact that the four particles are free,

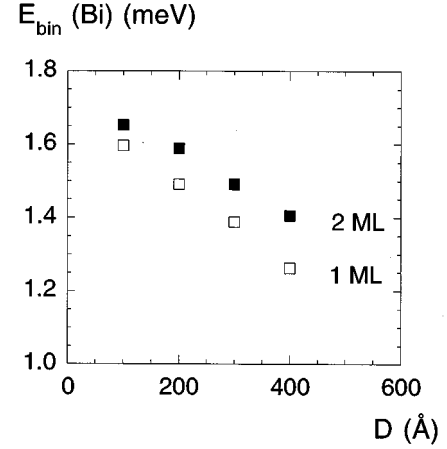


FIG. 3. Biexcitonic binding energy versus defect size D for defect depths of 1 and 2 ML.

whereas in our case the situation is much more complicated by the localization potential. This approach for biexcitons bound to interface defects corresponds to the first variational wave function for free QW biexcitons of Miller *et al.*² in the way that the correlation parts of the biexcitonic wave functions are the symmetrized products of the excitonic correlation terms. This approach is very crude because no repulsive difference appears in the wave function. This means that it contains no part for the repulsion that would disfavor the electron-hole configurations with highly repulsive Coulombic energies. Kleinman³ has corrected this deficiency by completing the first term, which includes the attractive coordinates by a term with repulsive coordinates. By this means he achieved an improvement of about 65% compared to the results of Miller *et al.* On the experimental side, the use of four-wave-mixing techniques provides an accurate experimental determination of the biexciton binding energy. The more recent experimental values¹³ are about the double of the values found by Kleinman. Thus a comparison of the results of Miller *et al.* with these experimental ones yields a factor 3 between them. Passing now to bulk biexcitons, one finds the results of Brinkman *et al.*,¹ who used the same wave function as Kleinman. A comparison between their results and the Green's-function Monte Carlo calculations of Lee *et al.*²⁴ shows a factor of about 1.6 between them. In summary, the best experimental and theoretical values for the free bulk and the free QW biexcitons differ by a factor between 2 and 3 from the trial wave function of Miller *et al.* This fact implies that a great care has to be exercised when discussing the binding energy of the localized biexciton. The latter is defined as the difference between 2 times the total exciton energy and the total biexciton energy:

$$E_{bin}(bi) = 2 E_{tot}(ex) - E_{tot}(bi). \quad (6)$$

This means, in practice, that we calculate the total biexciton energy using Ψ_{bi} for the biexciton Hamiltonian (4) and the total exciton energy using Ψ_{ex} for the exciton Hamiltonian (1). The resulting biexciton binding energy is presented in Fig. 3 for the same parameters as in Sec. II. The general behavior is a decreasing binding energy with increasing defect size. For a 1-ML defect depth the values decrease

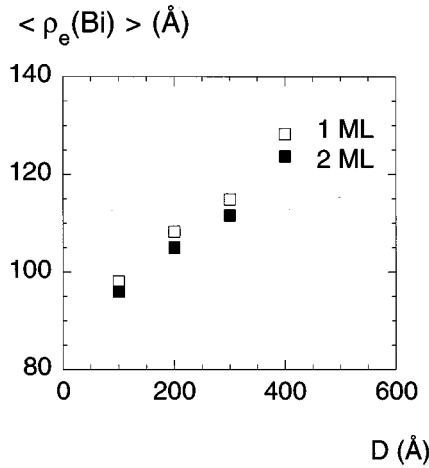


FIG. 4. Biexcitonic expectation value for the electron lateral distance from the defect center versus defect size D for defect depths of 1 and 2 ML.

monotonically from about 1.6 meV to 1.25 meV. The corresponding values for 2 ML are only approximately 0.1 meV higher.

Apparently, there exists a general relation between the size and the binding energy not only for the exciton but also for the biexciton. The biexciton binding energy seems to increase with decreasing biexciton size. On the experimental side, this has been confirmed for QW's by Birkedal *et al.*¹³ This trend was found in theoretical investigations for QWW's (Ref. 5) and for QD's (Ref. 9) with infinitely high barriers. In our case there are no infinitely high barriers that are responsible for a clearly defined localization. Nevertheless, the defect potential causes a localization, as already demonstrated for the excitons in Sec. II. The question whether a relation exists between the localization and the biexciton binding requires an investigation of the lateral size of the biexciton. Therefore, we calculate for the biexciton the mean distance between an electron and the center of the interface defect:

$$\langle \rho_e(\text{bi}) \rangle = \langle \Psi_{\text{bi}} | 1/2(\rho_{e1} + \rho_{e2}) | \Psi_{\text{bi}} \rangle. \quad (7)$$

The calculations show that the mean distances for the hole are nearly the same as those for the electron. As a consequence, $\langle \rho_e \rangle$ is a fair estimate of the lateral biexciton size. As presented in Fig. 4, $\langle \rho_e \rangle$ ranges from about 95 Å to 130 Å and shows a clear monotonic increase with increasing defect size for 1 and 2 ML. The values for the 2-ML defects are smaller than the values for the 1 ML due to the deeper localization potential. This means that the biexciton size (like the exciton size) is decreasing with decreasing defect size in this intermediate region while the biexciton binding energy increases. This is in agreement with the trends found in the QW, QWW, and QD structures cited above. The comparison between the exciton and the biexciton mean extensions shows that the latter is about 10–25 % greater. This translates to a biexciton volume that is about 20–50 % greater than the exciton one.

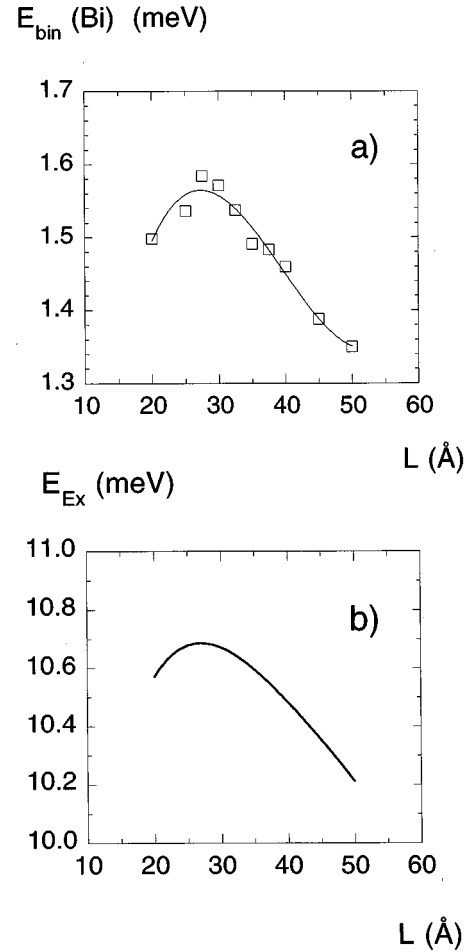


FIG. 5. (a) Biexciton binding energy versus well width L for a defect depth of 1 ML and $D=200$ Å. The numerical precision of the calculation (squares) is of the order of the distance to the curve that is a polynomial fit. (b) Binding energy of the *free* QW exciton versus well width L .

A second possibility of external influence on the localization consists in changing the well width. The results for the 1-ML defect depth and a defect size of 200 Å are presented in Fig. 5(a).

From 20 Å up to about 27.5 Å the binding energy is increasing and after a maximum value of about 1.6 meV the binding energy decreases with increasing well width. This well width dependence is reminiscent of the well-known binding energy of free QW excitons²⁵ and has been explained by the changing z -direction extension due to the finite-barrier heights. The corresponding values for our parameters are presented in Fig. 5(b). One clearly sees the same width dependence for the exciton as for the biexciton with a maximum value for about 27.5 Å. In fact, in our model, both the exciton and the biexciton wave functions are described in a separable form with the same parts χ_e and χ_h and consequently their z -direction extensions are the same. To get an idea of this extension we calculate $\langle z_{e,h}^2 \rangle$, which shows that the hole extension is a monotonical decreasing function with decreasing QW width. On the contrary, the extension of the electron is decreasing down to about 30 Å and then increasing with decreasing QW width due to the less efficient confinement of the finite well. In summary, we are able to show

TABLE I. Individual energies and the ratio of the attractive and the repulsive Coulomb energy. Calculations are given for the three-dimensional hydrogen, the two-dimensional hydrogen, the three-dimensional positronium molecule and the biexciton in the QW with $A=1$ ML and $D=200$ Å.

E (eV)	$H_2^{(3D)}$ ^a	$H_2^{(3D)}$ ^b	$H_2^{(2D)}$ ^c	$e^+e^+e^-e^-$ (3D) ^b	$h^+h^+e^-e^-$ (QW)
E_{kin}	30.99		142	13.12	
E_{att}	-97.20	-98.14	-426	-40.18	-59.4×10^{-3}
$E_{rep}(ee)$	15.59	15.75	68	6.51	11.4×10^{-3}
$E_{rep}(hh)$	18.66	18.22	74	6.51	12.2×10^{-3}
E_{tot}	-30.96		-142	-14.04	
E_{bin}	3.76		33	0.43	
E_{att}/E_{rep}	2.8	2.9	3.0	3.3	2.5

^aReference 26.

^bReference 14.

^cReference 27.

that the dependence of the bound biexciton binding energy on the QW width is coupled to the z -direction extension. Due to the fact that the values for $\langle z_e^2 \rangle$ and $\langle z_h^2 \rangle$ are significantly different, a direct attribution to a biexciton size for the z direction is not possible, unlike the case of the lateral size.

Finally, we consider the Coulomb energy, which consists of two repulsive and four attractive parts and can be simplified by reason of symmetry to the expression

$$E_{Coul} = \frac{e^2}{4\pi\epsilon_0\epsilon_r} \left\langle \frac{1}{|\vec{r}_{e1} - \vec{r}_{e2}|} \right\rangle + \frac{e^2}{4\pi\epsilon_0\epsilon_r} \left\langle \frac{1}{|\vec{r}_{h1} - \vec{r}_{h2}|} \right\rangle - 4 \times \frac{e^2}{4\pi\epsilon_0\epsilon_r} \left\langle \frac{1}{|\vec{r}_{e1} - \vec{r}_{h1}|} \right\rangle \quad (8)$$

where the first term on the right-hand side is equal to $E_{rep}(ee)$, the second term to $E_{rep}(hh)$ and the third term to E_{att} . In the following we analyze the ratio of the attractive E_{att} and the repulsive Coulomb energy $E_{rep} = E_{rep}(ee) + E_{rep}(hh)$. We start our discussion with some results from molecular physics in Table I. The hydrogen molecule was handled in an approximation by Flügge²⁶ in three dimensions and in the same way in two dimensions by Zhu *et al.*²⁷ We present also the recent three-dimensional results from Rebane and Zotev,¹⁴ for the hydrogen molecule and the positronium molecule.

We start with the limiting case of $\sigma = m_e/m_h = 0$, which is nearly satisfied for the hydrogen molecule H_2 . The three-dimensional results of Flügge show a ratio of 2.8, whereas the more accurate calculation by Rebane and Zotev does not considerably change this ratio E_{att}/E_{rep} . The comparison with the energies of the two-dimensional hydrogen molecule shows that the absolute energies are considerably enhanced: by about a factor 4 for the individual energies and a factor 8 for the binding energy. This strong enhancement of the binding energy for a reduction of the dimensionality is well known for free excitons, where the transition from three to two dimensions leads to a factor 4. On the other hand, the Coulomb energy ratio has only weakly changed to a value of 3.0. In the second limiting case of $\sigma = 1$, i.e., the positronium molecule, the three-dimensional calculation of Rebane and Zotev leads to a much greater extension accompanied by energy values that are about half those of the three-dimensional hydrogen. They obtained a ratio of the Coulomb

energies of 3.3. The corresponding two-dimensional calculation has been undertaken by Birkedal *et al.*¹³ They assumed a classical configuration where the holes and the electrons occupy the opposite corners of a square with a flexible size of the square. The symmetry of this geometric structure implicitly assumes that the particles have identical masses ($\sigma = 1$). They obtained a ratio E_{att}/E_{rep} of $2\sqrt{2}$ reflecting the square geometry. In summary, the cited calculations lead to a ratio between 2.8 and 3.3, which is only weakly dependent on the dimensionality and the mass ratio. This indicates that the ratio E_{att}/E_{rep} could play the role of a biexcitonic parameter, which provides, on the theoretical side, an estimate of the quality of the trial wave function.

For our case of the biexciton bound to the interface defect the ratio is presented in Fig. 6 versus the defect size. It corresponds to an in-plane mass ratio $\sigma_{xy} \approx 0.7$, which is closer to the positronium case than the hydrogen one.

Our calculations lead to ratios between 2.3 and 2.6, which are smaller than all the values cited in Table I. We attribute this to the missing suppleness of our biexciton trial wave function. This is in agreement with the above discussion of our wave function, which in no way takes the repulsive coordinates into account and should therefore decrease the ratio.

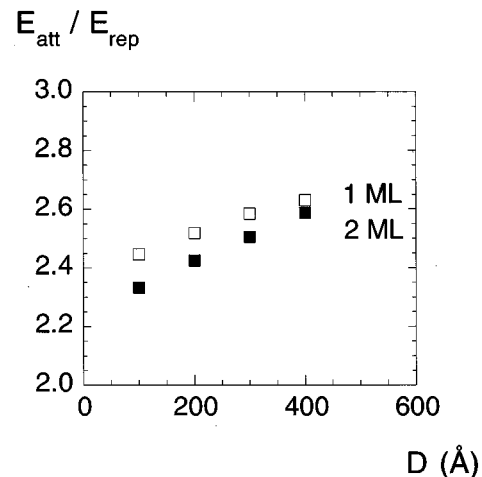


FIG. 6. Relation of the attractive to the repulsive Coulomb energy part versus defect size D for defect depths of 1 and 2 ML.

IV. CONCLUSION

We have studied the binding energy of biexcitons bound to single-island interface defects in deep QW's. Our variational wave function consisted in separate localization parts for each particle and a correlation part that corresponds to the one used by Miller *et al.*² By this means we have analyzed in detail the biexcitonic binding energy as a function of the defect size and the QW width. In order to estimate the biexciton extension we have calculated the lateral electron and hole extension. Our numerical results showed a clear correlation between the size of the biexciton and its binding energy. As in the case of the exciton, the biexciton binding energy increases with decreasing size.

The detailed analysis of the ratio E_{att}/E_{rep} for the free biexciton in different dimensions and with different mass ratios showed only weak differences. The comparison with the ratio for our trial wave function indicated that a better account of the repulsion between the like particles is required in our wave function. On the experimental side, Brunner *et al.*¹⁶ have found for a comparable $\text{Al}_x\text{Ga}_{1-x}\text{As}/\text{GaAs}$ structure a value of about 4.2 meV, which has been attributed to the biexciton. Thus further work is necessary to reconcile theory and experiment.

ACKNOWLEDGMENTS

The Laboratoire de Physique de la Matière Condensée ENS is Unité Associée au CNRS (UA 1437) et aux Univer-

sités Paris 6 et Paris 7. O.H. gratefully acknowledges the EEC for financial support (Training and Mobility of Researchers, Contract No. ERB FMB ICT 961 405).

APPENDIX

The following relation is often used:

$$e^{a \cos \varphi} = \sum_{n=-\infty}^{\infty} e^{in\varphi} I_n(a),$$

where I_n means the modified Bessel function and we define

$$I_{eh}(q) = \int \chi_e^2(z_e) \chi_h^2(z_h) e^{-q|z_e - z_h|} dz_e dz_h,$$

$$I_{ee}(q) = \int \chi_e^2(z_{e1}) \chi_e^2(z_{e2}) e^{-q|z_{e1} - z_{e2}|} dz_{e1} dz_{e2},$$

$$I_{hh}(q) = \int \chi_h^2(z_{h1}) \chi_h^2(z_{h2}) e^{-q|z_{h1} - z_{h2}|} dz_{h1} dz_{h2}.$$

1. Normalization

The normalization is completely analytical:

$$1 = \langle \Psi_{bi} | \Psi_{bi} \rangle = \langle \Psi_1 | \Psi_1 \rangle + \langle \Psi_2 | \Psi_2 \rangle + 2 \langle \Psi_1 | \Psi_2 \rangle \quad (\text{A1})$$

$$\begin{aligned} \langle \Psi_1 | \Psi_2 \rangle &= N^2 (2\pi)^4 \int d\varrho_{e1} d\varrho_{e2} d\varrho_{h1} d\varrho_{h2} e_{e1} e_{e2} e_{h1} e_{h2} e^{-2d_e(\varrho_{e1}^2 + \varrho_{e2}^2)} e^{-2d_h(\varrho_{h1}^2 + \varrho_{h2}^2)} \sum_n I_n \left(\frac{2}{\lambda^2} e_{e1} e_{h1} \right) \\ &\quad \times I_n \left(\frac{2}{\lambda^2} e_{e2} e_{h2} \right) I_n \left(\frac{2}{\lambda^2} e_{e1} e_{h2} \right) I_n \left(\frac{2}{\lambda^2} e_{e2} e_{h1} \right) \\ &= N^2 \frac{\pi^4}{d_e^2} \int d\varrho_{h1} d\varrho_{h2} e_{h1} e_{h2} \exp \left[- \left(2d_h - \frac{1}{d_e \lambda^4} \right) (\varrho_{h1}^2 + \varrho_{h2}^2) \right] \sum_n I_n^2 \left(\frac{1}{d_e \lambda^4} e_{h1} e_{h2} \right), \end{aligned}$$

$$\langle \Psi_1 | \Psi_2 \rangle = N^2 \frac{\pi^4 \lambda^4}{16 d_e d_h (d_e d_h \lambda^4 - 1)},$$

$$\langle \Psi_1 | \Psi_1 \rangle = \langle \Psi_2 | \Psi_2 \rangle$$

$$= N^2 \frac{\pi^4 \lambda^8}{16 (d_e d_h \lambda^4 - 1)^2},$$

$$d_{e,h} = 1/\lambda^2 + 1/\lambda_{e,h}^2.$$

2. Interface defect energy

The potential energy due to the binding to the interface defect leads to the expression

$$U_{def}(e) = \langle \Psi_{bi} | \mathcal{V}_{def}(e_1) + \mathcal{V}_{def}(e_2) | \Psi_{bi} \rangle$$

$$= 2[\langle \Psi_1 | \mathcal{V}_{def}(e_1) | \Psi_1 \rangle + \langle \Psi_2 | \mathcal{V}_{def}(e_1) | \Psi_2 \rangle$$

$$+ 2\langle \Psi_1 | \mathcal{V}_{def}(e_1) | \Psi_2 \rangle]$$

$$= 4[\langle \Psi_1 | \mathcal{V}_{def}(e_1) | \Psi_1 \rangle + \langle \Psi_1 | \mathcal{V}_{def}(e_1) | \Psi_2 \rangle]. \quad (\text{A2})$$

The integrals are of the same form as for the calculations of the normalization and are thus calculated analytically.

3. Coulomb energy

All Coulomb integrals can be analytically reduced to the following forms, which are finally calculated numerically ($i, j \in [1, 2]$):

$$\left\langle \Psi_i \left| \frac{1}{|\vec{r}_{e1} - \vec{r}_{h1}|} \right| \Psi_j \right\rangle = A_{ij} \int e^{-\alpha_{ij} q^2} I_{eh}(q) dq,$$

$$\left\langle \Psi_i \left| \frac{1}{|\vec{r}_{e1} - \vec{r}_{e2}|} \right| \Psi_j \right\rangle = B_{ij} \int e^{-\beta_{ij} q^2} I_{ee}(q) dq,$$

$$\left\langle \Psi_i \left| \frac{1}{|\vec{r}_{h1} - \vec{r}_{h2}|} \right| \Psi_j \right\rangle = C_{ij} \int e^{-\gamma_{ij} q^2} I_{hh}(q) dq.$$

4. Kinetic in-plane energy

The kinetic in-plane energy is the most difficult part of the Hamiltonian and has to be calculated numerically:

$$\begin{aligned} E_{kinxy} &= \langle \Psi_{bi} | \mathcal{T}_{xy} | \Psi_{bi} \rangle \\ &= \langle \Psi_{bi} | \mathcal{T}_{xy}(e_1) + \mathcal{T}_{xy}(e_2) + \mathcal{T}_{xy}(h_1) + \mathcal{T}_{xy}(h_2) | \Psi_{bi} \rangle \\ &= 4[\langle \Psi_1 | \mathcal{T}_{xy}(e_1) + \mathcal{T}_{xy}(h_1) | \Psi_1 \rangle + \langle \Psi_1 | \mathcal{T}_{xy}(e_1) + \mathcal{T}_{xy}(h_1) | \Psi_2 \rangle]. \end{aligned} \quad (A3)$$

We present the most difficult term of the kinetic energy:

$$\begin{aligned} \langle \Psi_1 | \mathcal{T}_{xy}(e_1) | \Psi_2 \rangle &= -\frac{\hbar^2}{2 m_{xy}(e)} \langle \Psi_1 | \vec{\nabla}_{\vec{e}_1}^2 | \Psi_2 \rangle \\ &= -\frac{\hbar^2 N^2}{2 m_{xy}(e)} \int d^2 \varrho_{e1} d^2 \varrho_{h1} d^2 \varrho_{e2} d^2 \varrho_{h2} \\ &\quad \times e^{-2/\lambda_e^2 (\varrho_{e1}^2 + \varrho_{e2}^2)} e^{-2/\lambda_h^2 (\varrho_{h1}^2 + \varrho_{h2}^2)} \\ &\quad \times e^{-(\vec{\varrho}_{e1} - \vec{\varrho}_{h1})^2 / \lambda^2} e^{-(\vec{\varrho}_{e2} - \vec{\varrho}_{h2})^2 / \lambda^2} \\ &\quad \times e^{-(\vec{\varrho}_{e1} - \vec{\varrho}_{h2})^2 / \lambda^2} e^{-(\vec{\varrho}_{e2} - \vec{\varrho}_{h1})^2 / \lambda^2} \\ &\quad \times \underbrace{[-4 d_e + 4 d_e^2 \varrho_{e1}^2 + 4 \varrho_{h2}^2 / \lambda^2]}_{\rightarrow T_1} + \underbrace{-8 \vec{\varrho}_{e1} \vec{\varrho}_{e2} d_e / \lambda^2}_{\rightarrow T_2}, \end{aligned}$$

$$\begin{aligned} T_1 &= -\frac{\hbar^2 N^2 \pi^2}{8 m_{xy}(e)} \frac{\lambda^4}{d_e d_h} \int dx_{e1} dx_{e2} dx_{h1} dx_{h2} \left[-4 d_e + 2 d_e^2 x_{e1}^2 + \frac{2}{d_h \lambda^4} x_{h2}^2 \right] \\ &\quad \times e^{-(x_{e1}^2 + x_{e2}^2 + x_{h1}^2 + x_{h2}^2) + \gamma(x_{e1} x_{h1} + x_{e2} x_{h2} + x_{e1} x_{h2} + x_{e2} x_{h1})} \sum_{n=-\infty}^{+\infty} \tilde{T}_n(\gamma x_{e1} x_{h1}) \tilde{T}_n(\gamma x_{e2} x_{h2}) \tilde{T}_n(\gamma x_{e1} x_{h2}) \tilde{T}_n(\gamma x_{e2} x_{h1}), \\ T_2 &= \frac{\hbar^2 N^2 \pi^2}{4 m_{xy}(e)} \frac{d_e \lambda^2}{\sqrt{d_e d_h}^3} \int dx_{e1} dx_{e2} dx_{h1} dx_{h2} x_{e1} x_{h2} e^{-(x_{e1}^2 + x_{e2}^2 + x_{h1}^2 + x_{h2}^2) + \gamma(x_{e1} x_{h1} + x_{e2} x_{h2} + x_{e1} x_{h2} + x_{e2} x_{h1})} \\ &\quad \times \sum_{n=-\infty}^{+\infty} \tilde{T}_n(\gamma x_{e1} x_{h1}) \tilde{T}_n(\gamma x_{e2} x_{h2}) \tilde{T}_n(\gamma x_{e2} x_{h1}) [\tilde{T}_{n-1}(\gamma x_{e1} x_{h2}) + \tilde{T}_{n+1}(\gamma x_{e1} x_{h2})], \\ \gamma &= 1/(\lambda^2 \sqrt{d_e d_h}). \end{aligned}$$

The terms T_1 and T_2 are calculated numerically using the bound and easy to handle functions \tilde{T}_n leading to a convergent sum in only a few terms:

$$\tilde{T}_n(x) := \sqrt{2 \pi x} e^{-x} I_n(x).$$

- ¹W. F. Brinkman, T. M. Rice, and B. Bell, *Phys. Rev. B* **8**, 1570 (1973).
- ²R. C. Miller, D. A. Kleinman, A. C. Gossard, and O. Munteanu, *Phys. Rev. B* **25**, 6545 (1982).
- ³D. A. Kleinman, *Phys. Rev. B* **28**, 871 (1983).
- ⁴L. Bányai, I. Galbraith, C. Ell, and H. Haug, *Phys. Rev. B* **36**, 6099 (1987).
- ⁵F. L. Madarasz, F. Szmulowicz, F. K. Hopkins, and D. L. Dorsey, *Phys. Rev. B* **49**, 13 528 (1994).
- ⁶T. Takagahara, *Phys. Rev. B* **39**, 10 206 (1989).
- ⁷G. W. Bryant, *Phys. Rev. B* **41**, 1243 (1990).
- ⁸L. Bányai, *Phys. Rev. B* **39**, 8022 (1989).
- ⁹Y. Z. Hu, M. Lindberg, and S. W. Koch, *Phys. Rev. B* **42**, 1713 (1990).
- ¹⁰A. Barenco and M. A. Dupertuis, *Phys. Rev. B* **52**, 2766 (1995).
- ¹¹Y. Z. Hu, S. W. Koch, M. Lindberg, N. Peyghambarian, E. L. Pollock, and F. F. Abraham, *Phys. Rev. Lett.* **64**, 1805 (1990).
- ¹²E. L. Pollock and S. W. Koch, *J. Chem. Phys.* **94**, 6776 (1991).
- ¹³D. Birkedal, J. Singh, V. G. Lyssenko, J. Erland, and J. M. Hvam, *Phys. Rev. Lett.* **76**, 672 (1996); J. Singh, D. Birkedal, V. G. Lyssenko, and J. M. Hvam, *Phys. Rev. B* **53**, 15 909 (1996).
- ¹⁴T. K. Rebane and V. S. Zotev, *Opt. Spectrosc.* **80**, 355 (1996).
- ¹⁵M. M. H. El-Gogary, M. A. Abdel-Raouf, M. Y. M. Hassan, and S. A. Saleh, *J. Phys. B* **28**, 4927 (1995).
- ¹⁶K. Brunner, G. Abstreiter, G. Böhm, G. Tränkle, and G. Weimann, *Phys. Rev. Lett.* **8**, 1138 (1994).
- ¹⁷F. Kreller, M. Lowisch, J. Puls, and F. Henneberger, *Phys. Rev. Lett.* **75**, 2420 (1995).
- ¹⁸T. Häuptl, H. Nickolaus, F. Henneberger, and A. Schülzgen, *Phys. Status Solidi B* **194**, 219 (1996).
- ¹⁹M. Sugawara, *Jpn. J. Appl. Phys., Part 1* **35**, 124 (1996).
- ²⁰Ph. Lelong, and G. Bastard, in *Proceedings of XXIII International Conference on the Physics of Semiconductors, Berlin, 1996*, edited by M. Scheffler and R. Zimmermann (World Scientific, Singapore, 1996), p. 1377.
- ²¹O. Heller and G. Bastard, *Phys. Rev. B* **54**, 5629 (1996).
- ²²G. Bastard, C. Delalande, M. H. Meynadier, P. M. Frijlink, and M. Voos, *Phys. Rev. B* **29**, 7042 (1984).
- ²³The analyzed structure differs a little from the one presented in this article: a hemispherical cap (lateral radius D and depth A) on a two-dimensional quantum well (width L) embedded in a great but finite cylinder. Ph. Lelong, and G. Bastard, in *Proceedings of the 12th International Conference on High Magnetic Fields in the Physics of Semiconductors II, Würzburg, 1996*, edited by G. Landwehr and W. Ossau (World Scientific, Singapore, 1997).
- ²⁴M. A. Lee, P. Vashishta, and R. K. Kalia, *Phys. Rev. Lett.* **51**, 2422 (1983).
- ²⁵R. L. Greene, K. K. Bajaj, and D. E. Phelps, *Phys. Rev. B* **29**, 1807 (1984).
- ²⁶S. Flügge, *Rechenmethoden der Quantentheorie*, (Springer-Verlag, Heidelberg, 1990).
- ²⁷J. Zhu, X. Chen, and J. -J. Xiong, *J. Phys., Condens. Matter* **3**, 9559 (1991).